Acta Mech
https://doi.org/10.1007/s00707-026-04734-1

ORIGINAL PAPER

Victor A. Eremeyev

Instability of the third-gradient beam

Received: 10 March 2026 / Revised: 17 April 2026 / Accepted: 23 April 2026
© The Author(s) 2026

Abstract We discuss the instability of a third-gradient beam, which is an inextensible elastic beam whose deformation energy depends on the first derivative of the curvature of its axis. Such one-dimensional problems arise from the homogenisation of slender, lengthy structures made of beam lattice metamaterials. The equation of equilibrium is derived using the Lagrange variational principle. Solutions to a few linear problems are presented. In addition to the linear analysis, we present an asymptotic solution for finite deformations, similar to those of Euler's elastica. We demonstrate the correspondence between the critical forces of third-gradient beams and those of classical Euler–Bernoulli beams.

1 Introduction

Stability of structures is an old and well-developed branch of mechanics. Starting with the well-known Euler elastica problem, the instability of beams has been studied in numerous papers and summarised in numerous books; see, for example, [1–6]. It should be noted that the engineering problem of the stability of slender elements motivated the development of the corresponding mathematical tools, such as the calculus of variations, the theory of bifurcations, and differential equations, among others. Despite its long history, the instability of beam-like structures remains a relevant topic. This is due to at least three reasons:

- Various types of loading including boundary conditions;
- Complex microstructure;
- Extension towards small scales.

Considering various types of loadings, it is worth mentioning the instability under follower forces, which leads to the theory of the stability of non-conservative systems [6–8]. More recent results on the instability of flexible beams with sliders provide interesting applications of configurational mechanics [9–13]. Another example is the stability of moving structures, such as axially moving ones [14].

In the case of beam-like elements with a complex internal structure, we can mention flexible, multifolded, or origami-type metamaterials, which can exhibit particular behaviour when they lose stability, see [15–20] and the references therein.

Current developments in nanotechnology result in an extension of classical mechanics to smaller scales. This necessitates modifying beam models to consider various generalised continuum models, such as micropolar, coupled stress, micromorphic media, strain gradient, and nonlocal elasticity [21–27]. Peridynamics, a particular case of a nonlocal model, should also be mentioned [28–30].

In fact, the discussed above three reasons of beam model extensions are connected to each other. They can even represent different sides of the same phenomenon. For example, at the nanoscale we have different

V. A. Eremeyev (✉)
Dipartimento di Ingegneria civile, ambientale e architettura, University of Cagliari, via Marengo, 2, 09-123 Cagliari, Italy
E-mail: victor.eremeev@unica.it; eremeyev.victor@gmail.com

Published online: 15 May 2026

kind of interactions including long-range forces (van der Waals, Casimir, electrostatic, and others) which could depend on the shape of a thin structure, see e.g. [31,32]. Continual models of origami-like structures may require generalised models such as strain gradient elasticity [33] as well as for some other discrete systems [18,34,35]. Nowadays it is well established that the strain gradient elasticity is relevant as an effective continuum model for composites with high contrast in material properties [36–40] as well as at small scales [41–43]. Within the strain gradient elasticity, a deformation energy depends on strain and higher-order gradients of displacements [44,45]. In this approach in addition to stresses, there are also hyper-stresses. From the point of view of beam mechanics, they are similar to bi-moment and double force in the theory of thin-walled beams [46–48]. In particular, recently even the third-gradient elasticity was used an effective medium for beam-like metamaterials [49–51], namely truss-like structures whose floppy modes correspond to circular mechanisms. Initially, the gradient elasticity of third order was proposed by Mindlin [52] for describing surface stresses. In the following, we also refer to [45,53–57] for the general gradient elasticity of third order. The gradient elasticity of third order, or of any other order, is a further extension of strain gradient elasticity developed by Toupin and Mindlin [58–61]. This model of the strain gradient elasticity of second order has been further developed by other researchers, leading to various modifications as in [42,62,63]. The buckling of beams in strain gradient elasticity has been studied in the literature, see e.g. [64–66]. This approach uses Toupin–Mindlin strain gradient elasticity or similar models as a starting point. Then, the corresponding one-dimensional beam model can be derived using standard Euler–Bernoulli or Timoshenko-type kinematics within a variational approach. Various models of nonlocal and strain gradient beams are summarised in [67]. The essential difference between these beam models and those in [49–51] is that, in the latter case, the deformation energy depends *only* on the curvature derivative, i.e. on the higher-order derivatives. This means that the high-order elastic moduli become *dominant*, as the others vanish. In the classic case, however, the high-order moduli are usually related to characteristic lengths, which are typically small (see, for example, [68–70] for a calculation using lattice models). Consequently, the critical force is entirely determined by the higher-order elastic modulus.

The remainder of the paper is organised as follows. Section 2 describes the in-plane kinematics of an extensible beam. Then, in Sect. 3, we introduce the deformation energy density. Here, the energy depends on the derivative of the beam curvature. Section 5 is devoted to deriving the equilibrium conditions using a variational approach. The central point of the paper is the linear analysis of stability, which is presented in Sect. 6. Here, we discuss loss of stability under various boundary conditions and compare it with that of classical Euler–Bernoulli beams. The variational derivation of critical forces is discussed in Sect. 7. Using dimensionless Rayleigh quotients, one can make a general comparison of critical forces, as discussed in Sect. 8. Bifurcation analysis (postbuckling) of a cantilever beam is provided in Sect. 9. Sections 10 and 11 are devoted to possible generalisations, including nth-order gradient beams. As an example, the instability of the fourth-order cantilever beam is analysed. Finally, we summarise the results and discuss future steps.

2 Kinematics

The in-plane deformations of an elastic beam can be described as a differentiable mapping from the initial reference placement to the current one. The reference placement can be described using the position vector, $\mathbf{R} = \mathbf{R}(S)$, where S is the referential arc-length parameter. Similarly, the current placement can be described using the position vector, denoted by $\mathbf{r} = \mathbf{r}(s)$, where s is the current arc-length parameter. We assume the inextensibility condition in the following, so $S = s$, allowing us to use the same arc-length parameter for both placements, $s \in [0, l]$. Here l is the beam length.

$$\mathbf{u} = \mathbf{r}(s) - \mathbf{R}(S) \equiv u(s)\mathbf{i}_1 + v(s)\mathbf{i}_2, \tag{1}$$

where $\mathbf{i}_1$, $\mathbf{i}_2$, and $\mathbf{i}_3$ are the unit vectors related to the Cartesian coordinates $x_1 = s$, x_2, and x_3, respectively, see Fig. 1. Since the beam is initially straight, the vector $\mathbf{R}$ is given by the simple formula $\mathbf{R} = s\,\mathbf{i}_1$.

The tangent vector $\boldsymbol{\tau}$ to the beam axis is given by the formula

$$\boldsymbol{\tau} = \mathbf{r}'(s), \tag{2}$$

where the prime stands for the derivative with respect to s, $(\ldots)' = \frac{\mathrm{d}}{\mathrm{d}s}$. It can be parameterised with the angle $\phi = \phi(s)$ as follows

$$\boldsymbol{\tau} = \cos\phi(s)\mathbf{i}_1 + \sin\phi(s)\mathbf{i}_2. \tag{3}$$

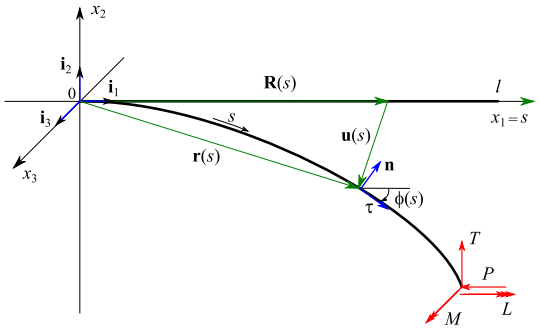

Fig. 1 Deformation of an elastic beam: reference and current placements

The curvature κ of the beam axis follows from the relations

$$\boldsymbol{\tau}' = \kappa \mathbf{n}, \quad \kappa = \phi', \quad \mathbf{n} = -\sin\phi(s)\mathbf{i}_1 + \cos\phi(s)\mathbf{i}_2, \tag{4}$$

where $\mathbf{n}$ is the unit normal to the beam axis. Let us note that due to the inextensibility of the beam we can use $\phi(s)$ as a primary descriptor instead of $\mathbf{r}$ or $\mathbf{u}$. Indeed, Eq. (3) takes the form

$$\mathbf{r}'(s) = \cos\phi(s)\mathbf{i}_1 + \sin\phi(s)\mathbf{i}_2, \quad \mathbf{u}'(s) = [\cos\phi(s) - 1]\mathbf{i}_1 + \sin\phi(s)\mathbf{i}_2. \tag{5}$$

For components of displacement vector, we get

$$u'(s) = \cos\phi(s) - 1, \quad v'(s) = \sin\phi(s). \tag{6}$$

Thus, $\mathbf{r}$ or $\mathbf{u}$ can be determined from ϕ up to constant vectors.

3 Constitutive relations

For a hyperelastic beam, we assume the existence of deformation energy. For a third-gradient beam, this energy takes the form given in [49–51]

$$W = W(\kappa'). \tag{7}$$

This distinguishes the model from the classical theory of beams, in which the deformation energy depends only on the curvature: $U = U(\kappa)$. To satisfy the material instability requirements (ellipticity conditions), we assume that

$$\frac{d^2 W}{d(\kappa')^2} > 0, \tag{8}$$

see [71–73] for ellipticity and material instabilities in strain gradient continua. In the following, we use the quadratic form for W:

$$W = \frac{1}{2} K (\kappa')^2, \tag{9}$$

where $K > 0$ is an elastic modulus. It can be calculated using the homogenisation technique, as described in [51]. Another linear third-gradient model was proposed for T-beams in [74].

4 Equilibrium conditions

We use the variational approach to derive the equilibrium equations. The equilibrium conditions follow from the stationarity of the total potential energy, $\mathcal{E}$. It takes the form:

$$\delta\mathcal{E}[\phi] = \delta \int_0^l W \,\mathrm{d}s - \delta V = 0, \tag{10}$$

where δV is the virtual work of external forces, moments, and double forces. For simplicity, we assume there are no external loadings distributed along the beam. Furthermore, we assume that the external loads are applied at the end $s = l$, while the point $s = 0$ remains fixed. Thus, δV is given by

$$\delta V = -P\delta u(l) + T\delta v(l) + M\delta\phi(l) + L\delta\phi'(l), \tag{11}$$

where P and T are tangential and transverse forces, respectively, M is a bending moment, and L is a double force as shown in Fig. 1. Since we will discuss possible instabilities, we will consider the compressive force P here.

First, using integration by parts, we obtain the formulas

$$\begin{aligned}
\delta \int_0^l W \,\mathrm{d}s &= \int_0^l \delta W \,\mathrm{d}s = \int_0^l K\kappa'\delta\kappa' \,\mathrm{d}s \\
&= -\int_0^l \left[K\kappa'\right]' \delta\kappa \,\mathrm{d}s + K\kappa'\delta\kappa\Big|_0^l \\
&= \int_0^l \left[K\kappa'\right]'' \delta\phi \,\mathrm{d}s - \left[K\kappa'\right]'\delta\phi\Big|_0^l + K\kappa'\delta\phi'\Big|_0^l.
\end{aligned} \tag{12}$$

At $s = 0$, we assume the kinematic boundary conditions, which are given by the following equations:

$$u(0) = 0, \quad v(0) = 0, \quad \phi(0) = 0, \quad \phi'(0) = 0. \tag{13}$$

Thus, we obtain

$$\delta u(0) = 0, \quad \delta v(0) = 0, \quad \delta\phi(0) = 0, \quad \delta\phi'(0) = 0. \tag{14}$$

From (6) and (13), it follows the relations:

$$u(l) = \int_0^l (\cos\phi - 1) \,\mathrm{d}s, \quad v(l) = \int_0^l \sin\phi \,\mathrm{d}s. \tag{15}$$

Consequently,

$$\delta u(l) = -\int_0^l \sin\phi\,\delta\phi \,\mathrm{d}s, \quad \delta v(l) = \int_0^l \cos\phi\,\delta\phi \,\mathrm{d}s, \tag{16}$$

Using Eqs. (12), (14), and (16), we came to the nonlinear boundary-value problem for a third-gradient beam

$$\left(K\phi''\right)'' - P\sin\phi + T\cos\phi = 0, \tag{17}$$

$$\phi\big|_{s=0} = 0, \quad \phi'\big|_{s=0} = 0, \tag{18}$$

$$-\left(K\phi''\right)'\big|_{s=l} = M, \quad K\phi''\big|_{s=l} = L. \tag{19}$$

Nonlinear theory can also be formulated in terms of displacements. First, the inextensibility condition takes the form of the equation

$$\sqrt{(1+u')^2+(v')^2}=1. \tag{20}$$

The angle and the curvature are given by the formulas

$$\phi=\arctan\left(\frac{v'}{1+u'}\right),\quad \kappa=\frac{(1+u')v''-v'u''}{\left[(1+u')^2+(v')^2\right]^{3/2}}. \tag{21}$$

The equilibrium conditions then follow from the stationarity of

$$\delta\mathcal{E}[u,v]=\delta\int_0^l W\,\mathrm{d}s-\delta V=0, \tag{22}$$

where u and v should satisfy the constraint condition. We can use the Lagrange multiplier technique for the constraint [75], which has some peculiarities for higher-order theories (see [76,77]). Obviously, the nonlinear formulation in displacements leads to more complex equations.

5 Linearised theory

By considering small angles, we can easily derive the linearised theory of third-gradient beams. The equilibrium equation now takes the form:

$$\left(K\phi''\right)''-P\phi+T=0, \tag{23}$$

which is supplemented by the combination of boundary conditions (18) and (19).

In the case of small deformations, the boundary-value problem can also be reformulated in terms of deflection, $v=v(s)$. Using the variational approach, we truncate the total potential energy up to quadratic terms. It has the form

$$\mathcal{E}=\frac{1}{2}\int_0^l K(\kappa')^2\,\mathrm{d}s+P\delta u(l)-T\delta v(l)-M\delta\phi(l)-L\delta\phi'(l).$$

Using the expansions

$$\sin\phi=\phi+O(\phi^3),\quad \cos\phi-1=-\frac{1}{2}\phi^2+O(\phi^2)$$

from (6) and (15), we obtain the following formulae up to quadratic terms

$$u'(s)=-\frac{1}{2}\phi^2(s),\quad v'(s)=\phi(s),\quad u(l)=-\frac{1}{2}\int_0^l\phi^2\,ds,\quad v(l)=\int_0^l\phi\,ds.$$

From these formulae, we can see that $u'=-\frac{1}{2}(v')^2$. Note that the inextensibility constraint given by (20) is satisfied up to quartic terms in this case. Since $\mathcal{E}$ becomes quadratic with respect to κ and ϕ, it is sufficient to consider them up to linear terms. From (21), we obtain that $\phi=v'$ and $\kappa=v''$. Thus, the total potential energy takes the form

$$\mathcal{E}[v]=\frac{1}{2}\int_0^l K(v''')^2\,\mathrm{d}s-\frac{1}{2}P\int_0^l(v')^2\,\mathrm{d}s-Tv'(l)-Lv''(l). \tag{24}$$

From the stationarity condition $\delta\mathcal{E} = 0$, we obtain the equilibrium equation

$$-\left(K v'''\right)''' + P v'' = 0, \tag{25}$$

and the natural boundary conditions at $s = l$

$$\delta v: \quad \left(K v'''\right)'' + P v' = 0, \tag{26}$$

$$\delta v': \quad -\left(K v'''\right)' = M, \tag{27}$$

$$\delta v'': \quad K v''' = L. \tag{28}$$

Note that, unlike in the Euler–Bernoulli beam model, the moment here is proportional to the fourth derivative of the deflection. The double force, which does not exist in classic beam theory, is proportional to the third derivative.

The kinematic (essential) boundary conditions at $s = 0$ are given by the following equations:

$$v = 0, \quad v' = 0, \quad v'' = 0. \tag{29}$$

These conditions are clearly geometrically defined: The deflection, angle of rotation, and curvature of the beam's axis all vanish. Obviously, one can consider various mixed boundary conditions.

6 Solution to some problems

Let us illustrate the instability of a homogeneous third-gradient beam under compressive force P, whereas $T = 0$, $M = 0$, and $L = 0$.

6.1 Cantilever beam

First, we will discuss a cantilever beam. Here, a cantilever beam is defined as a beam with one free end and one fixed end. The corresponding boundary-value problem is given by the following relations:

$$K\phi'''' - P\phi = 0, \tag{30}$$

$$\phi\big|_{s=0} = 0, \quad \phi'\big|_{s=0} = 0, \quad \phi''\big|_{s=l} = 0, \quad \phi'''\big|_{s=l} = 0. \tag{31}$$

From a physical point of view, these boundary conditions mean that the angle and curvature vanish at the left end, and the external moment and double force are zero at the right end.

First, we transform (30) into the dimensionless form by introducing parameters $\zeta = s/l \in [0, 1]$ and μ given by $\mu^4 = \frac{Pl^4}{K}$. As a result, we get the equation which contains only one parameter

$$\phi'''' - \mu^4\phi = 0, \tag{32}$$

where $(...)^{\cdot} = \frac{\mathrm{d}}{\mathrm{d}\zeta}$. This makes an essential difference between other gradient-type models [64–67], where a few material parameters are presented.

It has a solution in the form

$$\phi(\zeta) = C_1 \sinh(\mu\,\zeta) + C_2 \cosh(\mu\,\zeta) + C_3 \sin(\mu\,\zeta) + C_4 \cos(\mu\,\zeta), \tag{33}$$

where C_1, C_2, C_3, and C_4 are integration constants. Substituting (33) into non-dimensional form of (31), into the system

$$\phi\big|_{\zeta=0} = 0, \quad \phi^{\cdot}\big|_{\zeta=0} = 0, \quad \phi^{\cdot\cdot}\big|_{\zeta=1} = 0, \quad \phi^{\cdot\cdot\cdot}\big|_{\zeta=1} = 0,$$

we get a system of linear algebraic equations with respect to C_1, C_2, C_3, and C_4

$$\mathbb{A}\mathbb{C} = 0, \quad \mathbb{C} = (C_1, C_2, C_3, C_4)^T, \tag{34}$$

Table 1 Eigenvalues for the third-gradient and classic cantilever beams

k	μ_k	μ_{0k}
1	1.875104069	1.570796327
2	4.694091133	4.712388981
3	7.854757438	7.853981635
4	10.99554073	10.99557429
5	14.13716839	14.13716694
6	17.27875953	17.27875960
7	20.42035225	20.42035225
8	23.56194490	23.56194490
9	26.70353756	26.70353756
10	29.84513021	29.84513021

$$\mathbb{A} = \begin{bmatrix} 0 & 1 & 0 & 1 \\ 1 & 0 & 1 & 0 \\ \sinh\mu & \cosh\mu & -\sin\mu & -\cos\mu \\ \cosh\mu & \sinh\mu & -\cos\mu & \sin\mu \end{bmatrix}$$

The determinant of $\mathbb{A}$ has the form

$$\det\mathbb{A} = 2 + 2\cosh\mu\cos\mu. \tag{35}$$

Equation $\det\mathbb{A} = 0$ has an infinite series of roots μ_k, $k = 1, 2, \ldots$ Some roots are presented in Table 1.

The values of the kth critical force are given by the formula

$$P_k^* = \mu_k^4 \frac{K}{l^4}. \tag{36}$$

For relatively large k, μ_k can be approximated by the formula

$$\mu_k \approx \mu_{0k} = \frac{2k-1}{2}\pi.$$

Indeed, they almost coincide for $k \geq 7$, see Table 1. To prove this approximation, we can divide equation $\det\mathbb{A} = 0$ by $2\cosh\mu$ and obtain

$$\frac{1}{\cosh\mu} + \cos\mu = 0. \tag{37}$$

For relatively large values of μ, the first term in (37) becomes negligible, so it transforms into equation $\cos\mu = 0$, which has roots μ_{0k}.

It is interesting that this formula corresponds to the solution for a classic cantilever beam. In the case of a classic cantilever beam, we have the boundary-value problem:

$$\phi'''' + \mu_0^2\phi = 0, \quad \phi\big|_{\zeta=0} = 0, \quad \phi'\big|_{\zeta=1} = 0, \tag{38}$$

where $\mu_0 = Pl^2/D$, and $D = EI$ is the bending stiffness. E is the Young modulus and I is the second moment of area of the beam's cross section. The eigenvalues μ_{0k} of Eq. (38) follow from the equation

$$\cos\mu_0 = 0,$$

which has roots $\mu_{0k} = \frac{2k-1}{2}\pi$, $k = 1, 2, \ldots$, see e.g. [2] for details.

The minimal critical force for the third-gradient beam is given by the formula

$$P^* = \mu_1^4 \frac{K}{l^4} \approx 12.36236338\,\frac{K}{l^4}, \tag{39}$$

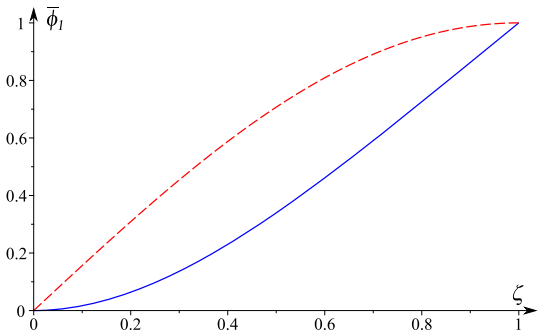

Fig. 2 Normalised eigen modes for the third-gradient cantilever beam (solid curve) and for the classic beam (dashed curve). Here $\bar{\phi} = \phi/\phi(1)$

whereas the classic formula reads

$$P_0^* = \mu_{01}^2 \frac{D}{l^2} \approx 2.467401101 \, \frac{D}{l^2}. \tag{40}$$

The next values of critical forces show significant growth compared to classical beams. Indeed, we have

$$P_k^* = \mu_k^4 \frac{K}{l^4} \sim k^4, \tag{41}$$

while

$$P_{0k}^* = \mu_{0k}^2 \frac{D}{l^2} \sim k^2, \tag{42}$$

Therefore, independently of the ratio K/Dl^2 we obtain that $P_k^* \gg P_{0k}^*$ when k exceeds a certain value.

The eigenmode has the following form

$$\phi_k(\zeta) = C \left[\sinh \mu\zeta - \sin \mu\zeta + \frac{(\sinh \mu + \sin \mu)\,(\cos \mu\zeta - \cosh \mu\zeta)}{\cosh \mu + \cos \mu} \right], \tag{43}$$

where C is an arbitrary constant and μ should be replaced by the corresponding eigenvalue μ_k. The graph of the first normalised eigenmode is given in Fig. 2 together with the buckling mode of the classic cantilever beam. The latter is given by the equation $\phi_{01} = \sin \mu_{01}\zeta$. For normalisation, we use the condition $\phi(1) = 1$. This gives us the following value of C in (43):

$$C = \frac{\cosh \mu + \cos \mu}{2 \, \sinh \mu \cos \mu - 2 \, \cosh \mu \sin \mu}. \tag{44}$$

Despite the similarity in the eigenvalues, we can see that the eigenmodes given in Fig. 2 behave differently. Similarly, one can solve other problems relating to the linear stability of third-gradient beams.

6.2 Clamped–clamped beam

Let us consider the case of clamped–clamped beam. In this case, the boundary conditions take the form

$$\phi\big|_{\zeta=0} = 0, \quad \phi^{\cdot}\big|_{\zeta=0} = 0, \quad \phi\big|_{\zeta=1} = 0, \quad \phi^{\cdot}\big|_{\zeta=1} = 0. \tag{45}$$

Substituting (45) into (33), we again obtain a system of linear algebraic equations with the matrix

$$\mathbb{A} = \begin{bmatrix} 0 & 1 & 0 & 1 \\ 1 & 0 & 1 & 0 \\ \sinh \mu & \cosh \mu & \sin \mu & \cos \mu \\ \cosh \mu & \sinh \mu & \cos \mu & -\sin \mu \end{bmatrix}.$$

Table 2 Eigenvalues for the third-gradient and classic clamped–clamped beams

k	μ_k	μ_{0k}
1	4.730040745	3.141592654
2	7.853204624	6.283185308
3	10.99560784	9.424777962
4	14.13716549	12.56637062
5	17.27875966	15.70796327
6	20.42035225	18.84955592
7	23.56194490	21.99114858
8	26.70353756	25.13274123
9	29.84513021	28.27433389
10	32.98672286	31.41592654

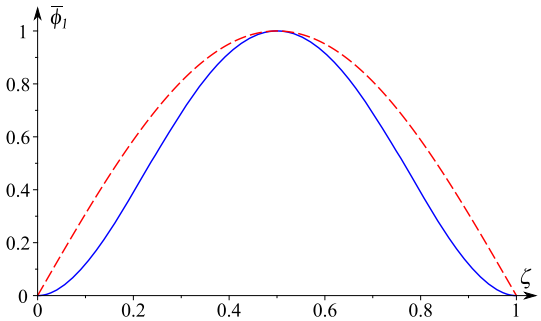

Fig. 3 Normalised eigen modes for the third-gradient clamped–clamped beam (solid curve) and for its classic counterpart (dashed curve). Here $\bar{\phi} = \phi/\phi(1/2)$

Its determinant is equal to

$$\det \mathbb{A} = 2 - 2\cosh\mu\cos\mu. \tag{46}$$

The comparison of the roots with the classic clamped–clamped beam is given in Table 2.

The critical forces are given by (36). The corresponding eigenmode has the form

$$\phi_k(\zeta) = C\left[\sinh\mu\zeta - \sin\mu\zeta + \frac{(\sinh\mu - \sin\mu)(\cos\mu\zeta - \cosh\mu\zeta)}{\cosh\mu - \cos\mu}\right], \tag{47}$$

where $\mu = \mu_k$ and C is an arbitrary constant. The first normalised eigenmode ϕ_1 is presented in Fig. 3 together with the classic solution, given by the formula $\phi_{01} = \sin\mu_{01}\zeta$. For normalisation, we assume that $\phi_1(1/2) = 1$, giving us the following expression for C:

$$C = \frac{\cos(\mu/2) + \cosh(\mu/2)}{-\sin(\mu/2)\cosh(\mu/2) + \cos(\mu/2)\sinh(\mu/2)}.$$

Let us recall that for the classical beam the roots are following from the equation $\sin\mu = 0$ and given by the formula $\mu_{0k} = \pi k$, see the third column in Table 2. As shown in Fig. 3, there are boundary effects near the beam ends (flattening at the ends).

6.3 "Simply supported" beam

In the following, by a simply supported beam we understand a beam with zero deflections at its ends, whereas other boundary conditions are natural ones and describe absence of concentrated moments and double force at the ends. In terms of deflection, the corresponding boundary conditions take the form

$$v(0) = v(l) = 0, \quad v'''(0) = v'''(l) = 0, \quad v''''(0) = v''''(l) = 0. \tag{48}$$

These boundary conditions mean that the deflection, external moment, and double force are all zero at the ends of the beam.

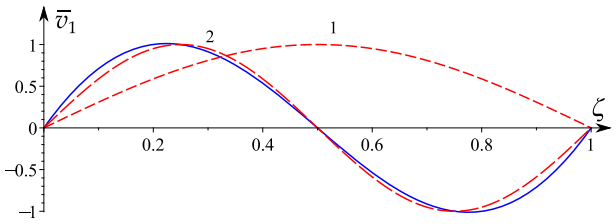

Fig. 4 Normalised eigen modes for the third-gradient simply supported beam (solid curve) and for its classic counterpart. Dashed curves 1 and 2 correspond to the first and second eigenmodes of the classic beams. Here $\bar{v}_1 = \bar{v}_1/\bar{v}(3/4)$

The non-dimensional form (25) transforms into

$$-\bar{v}^{\cdots\cdots} + \mu^4 \bar{v}^{\cdot\cdot} = 0, \tag{49}$$

with the boundary conditions

$$\bar{v}\big|_{\zeta=0} = \bar{v}\big|_{\zeta=1} = 0, \quad \bar{v}^{\cdots}\big|_{\zeta=0} = \bar{v}^{\cdots}\big|_{\zeta=1} = 0, \quad \bar{v}^{\cdots\cdot}\big|_{\zeta=0} = \bar{v}^{\cdots\cdot}\big|_{\zeta=1} = 0, \tag{50}$$

where $\bar{v} = v/l$. The general solution of (49) has the form

$$\bar{v}(\zeta) = C_1 \cosh(\mu\,\zeta) + C_2 \sinh(\mu\,\zeta) + C_3 \cos(\mu\,\zeta) + C_4 \sin(\mu\,\zeta) + C_5\zeta + C_6, \tag{51}$$

where $C_1 \ldots C_6$ are integration constants. Substituting (51) into (50), we get another linear system

$$\mathbb{B}\mathbb{C} = 0, \quad \mathbb{C} = (C_1, C_2, C_3, C_4, C_5, C_6)^T, \tag{52}$$

$$\mathbb{B} = \begin{bmatrix} 1 & 0 & 1 & 0 & 0 & 1 \\ 0 & 1 & 0 & -1 & 0 & 0 \\ 1 & 0 & 1 & 0 & 0 & 0 \\ \cosh\mu & \sinh\mu & \cos\mu & \sin\mu & 1 & 1 \\ \sinh\mu & \cosh\mu & \sin\mu & -\cos\mu & 0 & 0 \\ \cosh\mu & \sinh\mu & \cos\mu & \sin(\mu) & 0 & 0 \end{bmatrix}.$$

It is interesting that the determinant of $\mathbb{B}$ is given by the formula $\det\mathbb{B} = 2 - 2\cosh\mu\cos\mu$, i.e. coincides with (46). Thus, the eigenvalues and the critical forces are the same as in Sect. 6.2.

The eigenmodes have the form

$$\bar{v}_k(\zeta) = C\left[\cosh\mu\zeta - \cos\mu\zeta - \frac{\sinh\mu - \sin\mu}{\cosh\mu - \cos\mu}(\sinh\mu\zeta + \sin\mu\zeta)\right],$$

where again $\mu = \mu_k$ and C is an arbitrary constant. The first eigenmode is shown in Fig. 4 together with two classic eigenmodes, v_{01} and v_{02} (dashed curves 1 and 2, respectively), which are defined as $\bar{v}_{01} = \sin\pi\zeta$ and $\bar{v}_{02} = \sin 2\pi\zeta$. It has extremes at $\zeta = 1/4$ and $\zeta = 3/4$. For C, we used the value $C = 1/\max\limits_{\zeta\in[0,1]}|\bar{v}_1(\zeta)|$. Interestingly, there is no analogue to the first classic solution, i.e. $\bar{v}_{01}$. The first eigenmode for the third-gradient beam is similar to the second mode, $\bar{v}_{02}$. This difference can be explained by the fact that this eigenshape is suppressed by additional boundary conditions.

6.4 Simply supported–clamped beam

In this case, we have the following boundary conditions

$$v(0) = v(l) = 0, \quad v'''(0) = 0, \quad v''''(0) = 0, \quad v'(l) = 0, \quad v''(l) = 0. \tag{53}$$

Table 3 Eigenvalues for the third-gradient simply supported–clamped beam and their approximations

k	μ_k	μ_{0k}
1	4.395361068	4.712388981
2	7.706996051	7.853981635
3	10.89481256	10.99557429
4	14.06075244	14.13716694
5	17.21717448	17.27875960
6	20.36876854	20.42035225
7	23.51756429	23.56194490
8	26.66459307	26.70353756
9	29.81043449	29.84513021
10	32.95543950	32.98672287

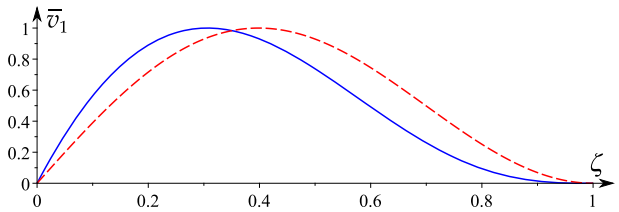

Fig. 5 Normalised eigen modes for the third-gradient simply supported–clamped beam (solid curve) and for its classic counterpart (dashed curve). Here $\bar{v} = v/\max_{s\in[0,1]} |v_1(s)|$.

Substituting (51) into (53), we obtain another linear system with a new matrix given by

$$\mathbb{B} = \begin{bmatrix} 1 & 0 & 1 & 0 & 0 & 1 \\ 0 & 1 & 0 & -1 & 0 & 0 \\ 1 & 0 & 1 & 0 & 0 & 0 \\ \cosh\mu & \sinh\mu & \cos\mu & \sin\mu & 1 & 1 \\ \mu\sinh\mu & \mu\cosh\mu & -\mu\sin\mu & \mu\cos\mu & 1 & 0 \\ s\cosh\mu & \sinh\mu & -\cos\mu & -\sin\mu & 0 & 0 \end{bmatrix}.$$

Its determinant is given by the formula

$$\det\mathbb{B} = (2\,\mu\,\cos\mu - 2\,\sin\mu)\cosh\mu - 2\,\sinh\mu\cos\mu + 2\,\mu.$$

Equation $\det\mathbb{B} = 0$ has a series of roots μ_k which could be approximated by the formula $\mu_{0k} = (2k+1)\pi/2$ for large k, $k = 1, 2, \ldots$, see Table 3.

The first eigenmode is shown in Fig. 5 together with its classical counterpart. Due to the additional boundary condition at the clamped end ($\zeta = 1$), the eigenmode is smoother than in the classic case.

6.5 Another mixed boundary condition

Note that, since there are three boundary conditions at one end of a third-gradient beam, there are more possible combinations of boundary conditions than in classic beam theory. For example, it is interesting to note that if we assume the following mixed boundary conditions

$$v(0) = v(l) = 0, \quad v''(0) = v''(l) = 0, \quad v''''(0) = v''''(l) = 0,$$

i.e. conditions which include the derivatives of even order, we obtain the eigenmode $\bar{v}_k = C_k \sin\mu_k\zeta$ which is exactly the same as for the classic simply supported beam with the eigenvalues followed from equation $\sin\mu l = 0$. Thus, for these boundary conditions we have a sequence of critical forces given by the exact formula

$$P_k^* = (\pi k)^4 \frac{K}{l^4}.$$

7 On variational derivation of critical forces

As in the case of classical beams or, more generally, in the case of self-adjoint ordinary differential equations, the critical force can be determined using the variational approach, see [75,78,79]. For the third-gradient beam, we introduce the Rayleigh quotient as follows

$$\mathcal{R}[\phi] = \frac{\int\limits_0^l K\left(\phi''\right)^2\, ds}{\int\limits_0^l \phi^2\, ds}. \tag{54}$$

The minimal critical force is then the minimum value of the Rayleigh quotient $\mathcal{R}[\phi]$ on the space of admissible functions V

$$P^* = \min_{\phi\in V} \mathcal{R}[\phi]. \tag{55}$$

The corresponding eigenfunction is the minimiser of the Rayleigh quotient $\mathcal{R}[\phi]$. Here V contains elements of the Sobolev space $H^2[0,l]$ that satisfy kinematic boundary conditions. Subsequent critical forces can be determined using the Rayleigh and Courant variational principles, as described in [78–81].

For example, let us consider a cantilever beam. Let us consider the test function given by the formula $\phi = 1/3\zeta^2(\zeta^2-4\zeta+6)$. This function satisfies the kinematic boundary conditions (31) at $\zeta = 0$ and takes the value 1 at $\zeta = 1$. By calculating the Rayleigh quotient, $\mathcal{R}[\phi]$, we obtain $\mu = 1.878853488$. Comparing it with μ_1 from Table 1 gives us a relative error of 0.2%, which seems to be acceptable for engineering applications.

For a clamped–clamped beam, we can use the test function $\phi = 16(1-\zeta)^2\zeta^2$. The result is $\mu = 4.738137221$. Comparing this value with μ_1 in Table 2 results in a relative error of 0.17%, which is also acceptable.

The Rayleigh quotient can also be expressed in terms of deflection

$$\mathcal{R}[v] = \frac{\int\limits_0^l K\left(v'''\right)^2\, ds}{\int\limits_0^l (v')^2\, ds}. \tag{56}$$

This results in

$$P^* = \min_{v\in V} \mathcal{R}[v], \tag{57}$$

where now V includes elements of the Sobolev space $H^3[0,l]$ satisfying kinematic boundary conditions.

8 Comparison with classic beams

We have demonstrated in Sect. 6 that there is a certain correspondence between eigenvalues μ_k and the eigenvalues μ_{0k} for the classical Euler–Bernoulli beams. Variational statement gives us a possibility to compare these models from a general point of view. The further analysis uses the standard comparison results discussed in [78–80] in more details. So in what follows we will provide this analysis in a brief way. First, we transform (54) and (56) in the dimensionless form

$$\mathcal{R}[\phi] = \frac{\int\limits_0^1 \left(\phi^{\bullet\bullet}\right)^2\, d\zeta}{\int\limits_0^1 \phi^2\, d\zeta}, \quad \mathcal{R}[v] = \frac{\int\limits_0^1 \left(v^{\bullet\bullet\bullet}\right)^2\, d\zeta}{\int\limits_0^1 (v^{\bullet})^2\, d\zeta}. \tag{58}$$

For classic beams, we introduce the corresponding Rayleigh quotients as follows

$$\mathcal{R}_0[\phi] = \frac{\int\limits_0^1 \left(\phi^{\cdot}\right)^2 \, ds}{\int\limits_0^1 \phi^2 \, ds}, \quad \mathcal{R}_0[v] = \frac{\int\limits_0^1 \left(v^{\cdot\cdot}\right)^2 \, ds}{\int\limits_0^1 \left(v^{\cdot}\right)^2 \, ds}. \tag{59}$$

Note that Eqs. (58) and (59) do not depend neither on elastic moduli nor the beam length.

Now the critical force can be determined from minimisation

$$\bar{P}^* = \min_{\phi \in V[\phi]} \mathcal{R}[\phi] \quad \text{or} \quad \bar{P}^* = \min_{v \in V[v]} \mathcal{R}[v], \tag{60}$$

where $V[\phi]$ and $V[v]$ contain elements of $H^2[0, 1]$ and $H^3[0, 1]$, respectively, satisfying kinematic boundary conditions, and

$$\bar{P}^* = \frac{l^4}{K} P^*.$$

For classical beams, we have similar formulae

$$\bar{P}_0^* = \min_{\phi \in S[\phi]} \mathcal{R}_0[\phi] \quad \text{or} \quad \bar{P}_0^* = \min_{v \in S[v]} \mathcal{R}_0[v], \tag{61}$$

where $S[\phi]$ and $S[v]$ includes elements of $H^1[0, 1]$ and $H^2[0, 1]$, respectively, which validate kinematic boundary conditions, and

$$\bar{P}_0^* = \frac{l^2}{D} P^*.$$

Therefore, one can see that the problem of comparison of critical forces is reduced to studies of relations of the norms in Sobolev's spaces.

As an example, let us consider a clamped–clamped beam. For the Euler–Bernoulli beam, the boundary conditions are $\phi(0) = \phi(1) = 0$. Thus, $S[\phi]$ coincides with $H_0^1[0, 1]$. For a third-gradient beam, however, there are additional boundary conditions, namely that the first derivative of the displacement at the endpoints be zero, $\phi'(0) = \phi'(1) = 0$. Thus, $V[\phi] = H_0^2[0, 1]$ and $V[\phi] \subset S[\phi]$. Note that for any element u of $H_0[0, 1]$ the Poincaré inequality holds [82, p. 24]

$$\|u\|_{L_2}^2 \leq \frac{1}{2} \|u'\|_{L_2}^2.$$

From this, it follows inequality

$$\|\phi'\|_{L_2}^2 \leq \frac{1}{2} \|\phi''\|_{L_2}^2.$$

Using this, we obtain the following:

$$R_0[\phi] \leq \frac{1}{2} R[\phi]$$

and

$$\bar{P}_0^* = \min_{\phi \in S[\phi]} R_0[\phi] \leq \min_{\phi \in V[\phi]} R_0[\phi] \leq \frac{1}{2} \min_{\phi \in V[\phi]} R[\phi] = \frac{1}{2} \bar{P}^*.$$

Thus, we came to relation $\bar{P}^* \geq 2\bar{P}_0^*$. This also follows from Table 2. Using Courant's minimax principle, we can also consider other values of critical forces.

9 Perturbation analysis

Unlike Euler's elastica problem, the straightforward integration of (17) leads to rather complex equations, see Appendix A. Nevertheless, we can apply classic perturbation technique as described in [83], see also [3,4,6]. First, we rewrite (17) with $T = 0$ as follows

$$\phi'''' - \lambda \sin\phi = 0, \quad \lambda = \mu^4. \tag{62}$$

Obviously, Eq. (62) supplemented by boundary conditions (31) always has a trivial (zero) solution $\phi_0 = 0$. We are now looking for a small, nontrivial solution to (62) and (31) in a series of a small parameter ϵ

$$\phi = \epsilon\phi_1 + \epsilon^2\phi_2 + \epsilon^3\phi_3 + \dots, \tag{63}$$

$$\lambda = \lambda_0 + \epsilon\lambda_1 + \epsilon^2\lambda_2 + \epsilon^3\lambda_3 + \dots, \tag{64}$$

Following the approach in [83], we can use the norm of the function ϕ, i.e. the maximum absolute value of the function over the interval, as a small parameter. Thus, we define

$$\epsilon = \max_{\zeta\in[0,1]} |\phi(\zeta)|.$$

From a physical point of view, ϕ takes its maximal value at the free end, i.e. at $\zeta = 1$. So we assume that

$$\epsilon = |\phi(1)|. \tag{65}$$

From (65), the so-called "false" boundary conditions follow

$$\phi_1(1) = 1, \quad \phi_k(1) = 0, \quad k > 1. \tag{66}$$

Substituting (63) and (64) into (62) and ordering the result with respect to ϵ^m, $m = 1, 2, \dots$, we obtain a series of problems

$$\epsilon: \ \phi_1'''' - \lambda_0\phi_1 = 0, \tag{67}$$

$$\epsilon^2: \ \phi_2'''' - \lambda_0\phi_2 = \lambda_1\phi_1, \tag{68}$$

$$\epsilon^3: \ \phi_3'''' - \lambda_0\phi_3 = \lambda_2\phi_1 + \lambda_1\phi_2 - \frac{1}{6}\lambda_0\phi_1^3, \tag{69}$$

$$\epsilon^4: \ \phi_4'''' - \lambda_0\phi_4 = \lambda_3\phi_1 + \lambda_2\phi_2 + \lambda_1\phi_3 - \frac{1}{6}\lambda_1\phi_1^3 - \frac{1}{2}\lambda_0\phi_2\phi_1^2, \tag{70}$$

$$\epsilon^5: \ \phi_5'''' - \lambda_0\phi_5 = \frac{\lambda_0\phi_1^5}{120} - \frac{1}{6}\lambda_2\phi_1^3 - \frac{1}{2}\lambda_0\phi_2^2\phi_1 - \frac{1}{2}\lambda_1\phi_2\phi_1^2 - \frac{1}{2}\lambda_0\phi_3\phi_1^2 + \lambda_1\phi_4 + \lambda_2\phi_3 + \lambda_4\phi_1 + \lambda_3\phi_2. \tag{71}$$

The first-order approximation (67) is exactly which we analyse in Sect. 6.1. It has a nonzero solution if $\lambda_0 = \mu_k^4$; otherwise, it has only a zero solution. In what follows, we consider the first eigenvalue (minimal critical force), so we set $\lambda_0 = \mu_1^4$. The corresponding eigenfunction ϕ_1 is given by (43) with normalisation constant C defined in (44).

Let us recall that the differential equation

$$\phi'''' - \lambda\phi = f(\zeta),$$

where $f(\zeta)$ is an arbitrary function, supplemented with necessary boundary conditions, is solvable for any f if λ is not the eigenvalue of a homogeneous problem, i.e. problem with $f = 0$. If λ is such an eigenvalue, it becomes solvable if and only if f is orthogonal to the eigenfunction ϕ_1

$$\int_0^1 f(\zeta)\phi_1(\zeta)\,d\zeta = 0. \tag{72}$$

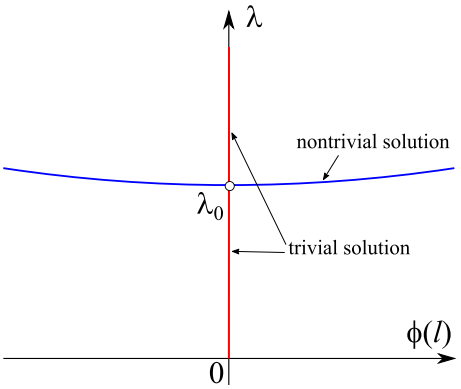

Fig. 6 Perturbation solution for the postbuckling

For example, considering the second-order approximation (68) we can see that it is solvable only if $\lambda_1 = 0$. Indeed, in this case condition (72) takes form

$$\lambda_1 \int_0^1 \phi_1^2(\zeta)\, d\zeta = 0.$$

Moreover, from (66) it follows that $\phi_2 = 0$.

With the previous results, Eq. (69) for the third approximation takes the form

$$\phi_3'''' - \lambda_0 \phi_3 = \lambda_2 \phi_1 - \frac{1}{6}\lambda_0 \phi_1^3.$$

The solvability condition (72) transforms into

$$\int_0^1 \left(\lambda_2 \phi_1 - \frac{1}{6}\lambda_0 \phi_1^3\right) \phi_1(\zeta)\, d\zeta = 0.$$

This gives us the value of λ_2

$$\lambda_2 = \frac{1}{6}\lambda_0 \frac{\int_0^1 \phi_1^4(\zeta)\, d\zeta}{\int_0^1 \phi_1^2(\zeta)\, d\zeta}. \tag{73}$$

Substituting the value $\lambda_0 = \mu_k^4$, Eqs. (43), and (44) into (73), we get

$$\lambda_2 = 1.209789442.$$

As in [83], we can calculate further approximations in the series (63) and (64). For example, Eq. (70) has now the form

$$\phi_4'''' - \lambda_0 \phi_4 = \lambda_3 \phi_1.$$

From (66) and (72), we obtain that $\lambda_3 = 0$ and $\phi_4 = 0$. Thus, the fourth approximation gives us only the trivial solution.

In what follows, we restrict ourselves to a quadratic terms in λ. Since λ_2 is positive, a new small nontrivial solution appears when $\lambda > \lambda_0$. When $\lambda < \lambda_0$, there is only the trivial solution $\phi = 0$. The point $(0, \lambda_0)$ is the bifurcation point. Thus, we obtain the classic bifurcation diagram shown in Fig. 6.

10 Instability of third-gradient beam of general type

Let us briefly discuss more general constitutive equations for an inextensible homogeneous third-gradient beam. The constitutive relation has the form

$$W = W(\kappa', \kappa) \tag{74}$$

with condition (8). Using ϕ as a kinematical descriptor, we obtain the following equilibrium equation

$$\frac{d^2}{ds^2}\frac{\partial W}{\partial \kappa'} - \frac{d}{ds}\frac{\partial W}{\partial \kappa} - P\sin\phi = 0. \tag{75}$$

Here we assumed that $T = 0$.

Linearisation of (75) in the vicinity of the straight shape $\phi = 0$ results in the equation

$$K\phi'''' - D\phi'' - P\phi = 0, \tag{76}$$

where

$$K = \left.\frac{\partial^2 W}{\partial(\kappa')^2}\right|_{\kappa=0,\kappa'=0}, \quad D = \left.\frac{\partial^2 W}{\partial \kappa^2}\right|_{\kappa=0,\kappa'=0}.$$

From (8), it follows that K is positive. Furthermore, if $K < 0$, then the linearised deformation energy is unbounded from below, see e.g. [73]. When expressed in terms of deflection v, Eq. (76) coincides with the equations presented in [64–66] up to notations.

The corresponding Rayleigh quotient takes the form

$$\mathcal{R}[\phi] = \frac{\int\limits_0^l \left[K\left(\phi''\right)^2 + D\left(\phi'\right)^2\right] ds}{\int\limits_0^l \phi^2\, ds}. \tag{77}$$

If D is positive, determining the critical forces becomes a routine procedure. Furthermore, by using Eq.(77) we can establish inequality

$$P^*_{Dk} \geq P^*_k, \quad k = 1, 2, \ldots$$

where the critical force, P^*_{Dk}, is calculated for $D > 0$, whereas the critical force, P^*_k, is calculated for $D = 0$.

In the case of negative D, the problem under consideration becomes more complex. For example, the loss of stability is possible if P is zero or even negative. For example, if $P = 0$, then Eq. (76) coincides with the classic beam equation up to notation if we treat D as a critical parameter. A similar problem arises in linear Toupin–Mindlin strain gradient elasticity if we assume that the Lamé moduli are not positive, see [73,84] for more details.

11 On instability of higher-order beams

Similarly, we can discuss the instability of higher-order beams. By a "higher-order beam", we mean a beam whose constitutive relation includes dependence on higher-order derivatives of curvature. We consider the following constitutive relation for a deformation energy

$$W = W(\kappa^{(n)}, \kappa^{(n-1)}, \kappa', \kappa), \tag{78}$$

where $n > 1$ is an integer. To prevent material instabilities, we can use the sufficient conditions

$$\frac{\partial^2 W}{\partial \kappa^{(n)2}} > 0. \tag{79}$$

The corresponding equilibrium equation has the form

$$\sum_{i=0}^{n}(-1)^{i+1}\frac{d^{i+1}}{ds^{i+1}}\left[\frac{\partial W}{\partial \kappa^{(i)}}\right]-P\sin\phi+T\cos\phi=0. \tag{80}$$

The linearisation of (80) results in a self-adjoint ordinary differential equation of order $2n+2$ in terms of ϕ. Its eigenvalues can be studied using the general technique, presented in, for example, [78–80]. In particular, if we assume the inequalities

$$\left.\frac{\partial^2 W}{\partial {\kappa^{(i)}}^2}\right|_{\kappa^{(n)}=0,\kappa^{(n-1)}=0,\kappa'=0,\kappa=0}\geq 0,\quad i=1,2\ldots,n-1,$$

in addition to (79), then we can prove the inequality for subsequent critical forces

$$P_k^{(i)}\geq P_k^{(i-1)},\quad i=1,2\ldots n,\quad k=1,2\ldots$$

where $P_k^{(i)}$ is the kth critical force calculated within the ith-gradient beam model.

11.1 Instability of a fourth-order gradient cantilever beam

For example, consider the instability of a cantilever beam under compressive force, where the deformation energy is taken in the form

$$W=\frac{G}{2}(\kappa'')^2, \tag{81}$$

where G is an elastic modulus. When $T=0$, Eq. (80) takes the form

$$G\phi^{(6)}+P\sin\phi=0. \tag{82}$$

Its linearisation results in

$$G\phi^{(6)}+P\phi=0. \tag{83}$$

We transform it into a dimensionless form

$$\phi^{\cdots\cdots}+\eta^6\phi=0, \tag{84}$$

where $\eta^6=Pl^6/G$. Its general solution is given by

$$\begin{aligned}\phi=&C_1\sin\eta\zeta+C_2\cos\eta\zeta+[C_3\cos(\eta\zeta/2)+C_5\sin(\eta\zeta/2)]\,\mathrm{e}^{-\sqrt{3}\,\eta\zeta/2}\\&+[C_4\cos(\eta\zeta/2)+C_6\sin(\eta\zeta/2)]\,\mathrm{e}^{\sqrt{3}\,\eta\zeta/2},\end{aligned} \tag{85}$$

where $C_1,\ldots C_6$ are integration constants.

For a cantilever beam, we assume the following boundary conditions

$$\begin{aligned}&\phi|_{\zeta=0}=0,\quad \phi^{\cdot}|_{\zeta=0}=0,\quad \phi^{\cdot\cdot}|_{\zeta=0}=0,\\&\phi^{\cdots}|_{\zeta=1}=0,\quad \phi^{\cdots\cdot}|_{\zeta=1}=0,\quad \phi^{\cdots\cdots}|_{\zeta=1}=0.\end{aligned}$$

Substituting (85) into these boundary conditions yields a system of linear algebraic equations for the integration constants. This system has a nontrivial solution if the determinant of the corresponding matrix vanishes, resulting in the equation:

$$\begin{aligned}&\mathrm{e}^{2\sqrt{3}\eta}\cos\eta+20\,\mathrm{e}^{\sqrt{3}\eta}\cos\eta\,(\cos(\eta/2))^2+16\,\sin\eta\sin(\eta/2)\cos(\eta/2)\,\mathrm{e}^{\sqrt{3}\eta}\\&\quad+8\,\cos(\eta/2)\,\mathrm{e}^{3/2\sqrt{3}\eta}-2\,\cos\eta\,\mathrm{e}^{\sqrt{3}\eta}+8\,\mathrm{e}^{\sqrt{3}/2\eta}\cos(\eta/2)+\cos\eta=0.\end{aligned} \tag{86}$$

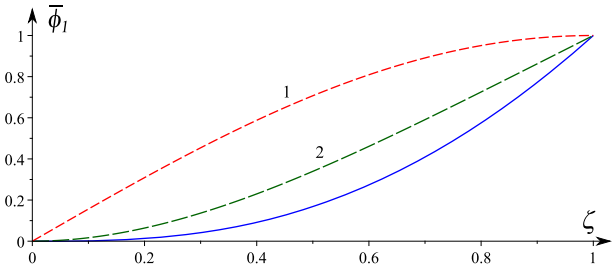

Fig. 7 Normalised eigen modes for the fourth-gradient cantilever beam (solid curve), for the classic beam (dashed curve 1), and for the third-gradient beam (curve 2). Here $\bar{\phi} = \phi/\phi(1)$

The first ten roots η_k, $k = 1, \dots 10$, of this equation are listed below

$$2.224772, \quad 4.802657, \quad 7.847647, \quad 10.995160, \quad 14.137194,$$

$$17.278761, \quad 20.420352 \quad 23.561944, \quad 26.703537, \quad 29.845130.$$

The corresponding critical force can be found using the formula $P_k^* = G\eta_k^6/l^6$, where the shape of the first eigenmode is presented in Fig. 7. This figure also presents the classic case (curve 1) and the case of the third-order gradient beam (curve 2). All curves are normalised using the condition $\phi(1) = 1$. It can be seen that the flattening of the solution near the clamped end increases as the order of the beam model increases.

12 Conclusions

This paper discusses the instability of third-gradient beams. In this model, the deformation energy depends on the curvature derivative. This constitutive equation emerges from the "continualisation" of discrete structures, as described in references [49–51]. The corresponding equilibrium equation, expressed in terms of displacements, is of sixth order. Note that six-order equations of statics are known in the literature on composite and three-layered beams, as discussed in the recent review [85]. Another approach that leads to similar equations for beams is based on 3D strain gradient elasticity, see e.g. [64–66]. However, the nature of these higher-order terms is generally different. Here, we present the derivation of equilibrium conditions and their linearisation, as well as solutions to some problems. Using the variational approach, we compared the values of the critical forces with those of the classical Euler–Bernoulli beam theory. As an example of postbuckling analysis, we considered a perturbation technique for a cantilever beam. We also briefly discussed the instability of higher-order beams. As one can see, the Euler–Bernoulli beam theory can be relatively easily extended to third-gradient beams.

The presented results could be extended to more complex cases of constitutive relations. In particular, the phenomena of material instability and structural buckling could be studied simultaneously. This is important for studying slender, long beam lattice structures. Indeed, such beam lattice metamaterials may exhibit local instabilities. A typical example of this is the behaviour of elastomer open-cell foams [86]. Various instability phenomena within the generalised models derived from discrete structures are discussed in [35,62,87–89]. Some lengthy structures made of beam lattice metamaterials demonstrate essential stretching, see, for example, [15–20,36,90,91]. Thus, we can consider models for higher-order extensible beams, including coupling between bending and stretching. Another possible extension of beam stability analysis is considering thermal or electromagnetic couplings, as in [92–94].

Open Access This article is licensed under a Creative Commons Attribution 4.0 International License, which permits use, sharing, adaptation, distribution and reproduction in any medium or format, as long as you give appropriate credit to the original author(s) and the source, provide a link to the Creative Commons licence, and indicate if changes were made. The images or other third party material in this article are included in the article's Creative Commons licence, unless indicated otherwise in a credit line to the material. If material is not included in the article's Creative Commons licence and your intended use is not permitted by statutory regulation or exceeds the permitted use, you will need to obtain permission directly from the copyright holder. To view a copy of this licence, visit http://creativecommons.org/licenses/by/4.0/.

Author contributions The manuscript was written by a single author.

Funding Open access funding provided by Università degli Studi di Cagliari within the CRUI-CARE Agreement. This work has been supported by the project "Metamaterials design and synthesis with applications to infrastructure engineering" funded by the MUR Progetti di Ricerca di Rilevante Interesse Nazionale (PRIN) Bando 2022 – grant 20228CPHN5, Italy.

Data availability No datasets were generated or analysed during the current study.

Declarations

Conflict of interest The authors declare no conflict of interest.

Appendix A First integral of the nonlinear system

First, let us assume that $K = \text{const}$ and $T = 0$. Then, multiplying Eq. (17) by ϕ' integrating the result gives

$$\left(K\phi'''' - P\sin\phi\right)\phi' = \left[K\left(\phi'\phi''' - \frac{1}{2}(\phi'')^2\right) + P\cos\phi\right]' = 0.$$

We can then obtain the first integral in the form

$$K\left[\phi''' - \frac{1}{2}(\phi'')^2\right] + P\cos\phi = C, \tag{A1}$$

where C is an integration constant. It can be determined from the boundary conditions. For example, for a cantilever beam we have $\phi''(l) = 0$ and $\phi'''(l) = 0$ at its free end. Substituting these formulas into (A1) at $s = l$, we find that

$$C = P\cos\phi(l).$$

This first integral could be useful for evaluating the accuracy of numerical calculations, for example. Further integration can be performed as described in [95, p. 638]. It results in the non-autonomous ordinary differential equation which solution could be represented in a parametric form [95, pp. 264, 265].

References

1. Love, A.E.H.: A Treatise on the Mathematical Theory of Elasticity, 4th edn. Dover, New York (1944)
2. Timoshenko, S.P., Gere, J.M.: Theory of Elastic Stability. McGrow-Hill, Auckland (1961)
3. Thompson, J.M.T., Hunt, G.W.: A General Theory of Elastic Stability. John Wiley & Sons, London (1973)
4. Antman, S.S.: Nonlinear Problems of Elasticity, 2nd edn. Springer, New York (2005)
5. Vetyukov, Y.: Nonlinear Mechanics of Thin-Walled Structures: Asymptotics. Direct Approach and Numerical Analysis. Springer, Vienna (2014)
6. Luongo, A., Ferretti, M., Di Nino, S.: Stability and Bifurcation of Structures: Statical and Dynamical Systems. Springer, Cham (2023)
7. Bolotin, V.V.: Nonconservative Problems of Theory of Elastic Stability. Pergamon Press, Oxford (1963)
8. Bigoni, D., Kirillov, O. (eds.): Dynamic Stability and Bifurcation in Nonconservative Mechanics. Springer, Cham (2019)
9. Bigoni, D., Bosi, F., Dal Corso, F., Misseroni, D.: Instability of a penetrating blade. J. Mech. Phys. Solids **64**, 411–425 (2014)
10. Bigoni, D., Bordignon, N., Piccolroaz, A., Stupkiewicz, S.: Bifurcation of elastic solids with sliding interfaces. Proceedings of the Royal Society A: Mathematical, Physical and Engineering Sciences **474**(2209) (2018)
11. Cazzolli, A., Misseroni, D., Dal Corso, F.: Elastica catastrophe machine: theory, design and experiments. J. Mech. Phys. Solids **136**, 103735 (2020)
12. Cazzolli, A., Dal Corso, F.: The elastica sling. European Journal of Mechanics-A/Solids **105**, 105273 (2024)
13. Neukirch, S., Dal Corso, F., Vetyukov, Y.: The frictionless flexible sliding sleeve. Journal of the Mechanics and Physics of Solids, 106330 (2025)
14. Scheidl, J., Vetyukov, Y.: Review and perspectives in applied mechanics of axially moving flexible structures. Acta Mech. **234**, 1331–1364 (2023)
15. Bertoldi, K., Vitelli, V., Christensen, J., Van Hecke, M.: Flexible mechanical metamaterials. Nat. Rev. Mater. **2**(11), 1–11 (2017)
16. Melancon, D., Forte, A.E., Kamp, L.M., Gorissen, B., Bertoldi, K.: Inflatable origami: Multimodal deformation via multistability. Adv. Func. Mater. **32**(35), 2201891 (2022)
17. Berinskii, I., Eremeyev, V.A.: On dynamics of origami-inspired rod. Int. J. Eng. Sci. **193**, 103944 (2023)
18. Berinskii, I., Eremeyev, V.A.: On the continuum modeling of the foldable rod with rigid links. Mechanics Research Communications, 104574 (2025)

19. Paradiso, M., Dal Corso, F., Bigoni, D.: A nonlinear model of shearable elastic rod from an origami-like microstructure displaying folding and faulting. J. Mech. Phys. Solids **200**, 106100 (2025)
20. Dudek, K.K., Kadic, M., Coulais, C., Bertoldi, K.: Shape-morphing metamaterials. Nat. Rev. Mater. **10**(10), 783–798 (2025)
21. Thai, H.-T.: A nonlocal beam theory for bending, buckling, and vibration of nanobeams. Int. J. Eng. Sci. **52**, 56–64 (2012)
22. Challamel, N., Wang, C.M., Reddy, J.N., Faghidian, S.A.: Equivalence between micromorphic, nonlocal gradient, and two-phase nonlocal beam theories. Acta Mech. **236**(2), 871–902 (2025)
23. Challamel, N., Kocsis, A., Wang, C.: Discrete and non-local elastica. Int. J. Non-Linear Mech. **77**, 128–140 (2015)
24. Wang, C.M., Gao, R.P., Zhang, H., Challamel, N.: Treatment of elastically restrained ends for beam buckling in finite difference, microstructured and nonlocal beam models. Acta Mech. **226**(2), 419–436 (2015)
25. Wang, C.M., Zhang, H., Challamel, N., Xiang, Y.: Buckling of nonlocal columns with allowance for selfweight. J. Eng. Mech. **142**(7), 04016037 (2016)
26. Barretta, R., Fabbrocino, F., Luciano, R., De Sciarra, F.M., Ruta, G.: Buckling loads of nano-beams in stress-driven nonlocal elasticity. Mech. Adv. Mater. Struct. **27**(11), 869–875 (2020)
27. Storch, J., Elishakoff, I.: Buckling of axially graded nonlocal columns: Closed-Form solutions. AIAA J. **59**(3), 1119–1124 (2021)
28. Naumenko, K., Yang, Z.: First order shear deformation beam theories in a peridynamic framework. Eur. J. Mech. A. Solids **112**, 105633 (2025)
29. Challamel, N., Zingales, M.: Two-phase peridynamic elasticity with exponential kernels. II: bending, buckling, and vibration of beams. J. Eng. Mech. **151**(5), 04025014 (2025)
30. Yang, Z., Naumenko, K., Altenbach, H., Ma, C.-C., Oterkus, E., Oterkus, S.: Beam buckling analysis in peridynamic framework. Arch. Appl. Mech. **92**(12), 3503–3514 (2022)
31. Mikhasev, G., Radi, E., Misnik, V.: Pull-in instability analysis of a nanocantilever based on the two-phase nonlocal theory of elasticity. Journal of Applied and Computational Mechanics **8**(4), 1456–1466 (2022)
32. Mikhasev, G., Radi, E., Misnik, V.: Modeling pull-in instability of cnt nanotweezers under electrostatic and van der Waals attractions based on the nonlocal theory of elasticity. Int. J. Eng. Sci. **195**, 104012 (2024)
33. Eremeyev, V.A., Berinskii, I.: On dynamics of origami-like structures: Necessity of enhanced models. Composite Structures, 119798 (2025)
34. Andrianov, I.V., Awrejcewicz, J.: Continuous models for 1D discrete media valid for higher-frequency domain. Phys. Lett. A **345**(1–3), 55–62 (2005)
35. Eremeyev, V.A., Berinskii, I.: Positive definiteness of deformation energy as a consistency condition of discrete-to-continuum transition. Continuum Mech. Thermodyn. **38**(1), 1–14 (2026)
36. Alibert, J.-J., Seppecher, P., dell'Isola, F.: Truss modular beams with deformation energy depending on higher displacement gradients. Math. Mech. Solids **8**(1), 51–73 (2003)
37. Rahali, Y., Giorgio, I., Ganghoffer, J.F., dell'Isola, F.: Homogenization à la Piola produces second gradient continuum models for linear pantographic lattices. Int. J. Eng. Sci. **97**, 148–172 (2015)
38. Abdoul-Anziz, H., Seppecher, P.: Strain gradient and generalized continua obtained by homogenizing frame lattices. Mathematics and Mechanics of Complex Systems **6**(3), 213–250 (2018)
39. dell'Isola, F., Steigmann, D.J.: Discrete and Continuum Models for Complex Metamaterials. Cambridge University Press, Cambridge (2020)
40. Andrianov, I.V., Danishevskyy, V.V., Kaplunov, J.: Low-frequency vibrations of a high-contrast orthotropic lattice. Mech. Res. Commun. **144**, 104386 (2025)
41. Cordero, N.M., Forest, S., Busso, E.P.: Second strain gradient elasticity of nano-objects. J. Mech. Phys. Solids **97**, 92–124 (2016)
42. Aifantis, E.C.: Gradient deformation models at nano, micro, and macro scales. J. Eng. Mater. Technol. **121**(2), 189–202 (1999)
43. Aifantis, E.C.: A concise review of gradient models in mechanics and physics. Frontiers in Physics **7**, 239 (2020)
44. Bertram, A., Forest, S. (eds.): Mechanics of Strain Gradient Materials. Springer, Cham (2020)
45. Bertram, A.: Compendium on Gradient Materials. Springer, Berlin (2024). Chapter on finite third-order gradient elasticity
46. Vlasov, V.Z.: Thin-walled Elastic Rods (in Russian). English Translation (1961). Published for NSF and Department of Commerce by the Israel Program of Scientific Translations, Jerusalem. Gosstroyizdat, Moscow (1940)
47. Simo, J.C., Vu-Quoc, L.: A geometrically-exact rod model incorporating shear and torsion-warping deformation. Int. J. Solids Struct. **27**(3), 371–393 (1991)
48. Ziegler, F.: Mechanics of Solids and Fluids. Springer, New Yourk (1991)
49. dell'Isola, F., Moschini, S., Turco, E.: Towards the synthesis of planar beams whose deformation energy depends on the third gradient of displacement. Mathematics and Mechanics of Complex Systems **12**(4), 573–597 (2024)
50. Terranova, L.M., Turco, E., Misra, A., dell'Isola, F.: Computational identification of double-bending stiffness: from Zigzagged Articulated Parallelograms with Articulated Braces (ZAPAB) structures to pure-curvature gradient planar inextensible 1D continua. Comptes Rendus. Mécanique **353**(G1), 647–672 (2025)
51. Rizzi, N.L., Seppecher, P., dell'Isola, F.: A third-gradient 1D continuum obtained via asymptotic expansion from a microstructure obtained constraining a sequence of modified Hart's antiparallelograms. Mathematics and Mechanics of Solids, 10812865251386767 (2026)
52. Mindlin, R.D.: Second gradient of strain and surface-tension in linear elasticity. Int. J. Solids Struct. **1**(4), 417–438 (1965)
53. Fedele, R.: Deformation-induced coupling of the generalized external actions in third-gradient materials. Z. Angew. Math. Phys. **73**(5), 218 (2022)
54. Fedele, R.: Third-gradient continua: nonstandard equilibrium equations and selection of work conjugate variables. Math. Mech. Solids **27**(10), 2046–2072 (2022)
55. Krawietz, A.: The crust shell and the edge beams of third-gradient continua in current and referential description. Acta Mech. **234**, 4141–4165 (2023)

56. dell'Isola, F., Fedele, R.: Irreducible representation of surface distributions and Piola transformation of external loads sustainable by third gradient continua. Comptes Rendus. Mécanique **351**(S3), 1–30 (2023)
57. Eremeyev, V.A., Lebedev, L.P., Cloud, M.J.: On admissible external loadings within the first and second strain gradient elasticity. Math. Mech. Solids **31**(2), 217 (2025)
58. Toupin, R.A.: Elastic materials with couple-stresses. Arch. Ration. Mech. Anal. **11**(1), 385–414 (1962)
59. Toupin, R.A.: Theories of elasticity with couple-stress. Arch. Ration. Mech. Anal. **17**(2), 85–112 (1964)
60. Mindlin, R.D.: Micro-structure in linear elasticity. Arch. Ration. Mech. Anal. **16**(1), 51–78 (1964)
61. Mindlin, R.D., Eshel, N.N.: On first strain-gradient theories in linear elasticity. Int. J. Solids Struct. **4**(1), 109–124 (1968)
62. Askes, H., Aifantis, E.C.: Gradient elasticity in statics and dynamics: an overview of formulations, length scale identification procedures, finite element implementations and new results. Int. J. Solids Struct. **48**(13), 1962–1990 (2011)
63. Aifantis, E.C.: Gradient material mechanics: perspectives and prospects. Acta Mech. **225**(4–5), 999–1012 (2014)
64. Lazopoulos, A.K., Lazopoulos, K.A., Palassopoulos, G.: Nonlinear bending and buckling for strain gradient elastic beams. Appl. Math. Model. **38**(1), 253–262 (2014)
65. Yaghoubi, S.T., Mousavi, S.M., Paavola, J.: Buckling of centrosymmetric anisotropic beam structures within strain gradient elasticity. Int. J. Solids Struct. **109**, 84–92 (2017)
66. Papargyri-Beskou, S., Tsepoura, K.G., Polyzos, D., Beskos, D.E.: Bending and stability analysis of gradient elastic beams. Int. J. Solids Struct. **40**(2), 385–400 (2003)
67. Chen, J.: Nonlocal Euler-Bernoulli Beam Theories: A Comparative Study. Springer, Cham (2021)
68. Maranganti, R., Sharma, P.: A novel atomistic approach to determine strain-gradient elasticity constants: Tabulation and comparison for various metals, semiconductors, silica, polymers and the (ir) relevance for nanotechnologies. J. Mech. Phys. Solids **55**(9), 1823–1852 (2007)
69. Admal, N.C., Marian, J., Po, G.: The atomistic representation of first strain-gradient elastic tensors. J. Mech. Phys. Solids **99**, 93–115 (2017)
70. Lazar, M., Agiasofitou, E., Böhlke, T.: Mathematical modeling of the elastic properties of cubic crystals at small scales based on the Toupin-Mindlin anisotropic first strain gradient elasticity. Continuum Mech. Thermodyn. **34**(1), 107–136 (2022)
71. Eremeyev, V.A.: Strong ellipticity conditions and infinitesimal stability within nonlinear strain gradient elasticity. Mech. Res. Commun. **117**, 103782 (2021)
72. Eremeyev, V.A.: Strong ellipticity and infinitesimal stability within nth-order gradient elasticity. Mathematics **11**(4), 1024 (2023)
73. Eremeyev, V.A.: On the ellipticity of static equations of strain gradient elasticity and infinitesimal stability. Vestnik St. Petersburg University, Mathematics 56(1), 77–83 (2023)
74. Vardoulakis, I., Giannakopoulos, A.E.: An example of double forces taken from structural analysis. Int. J. Solids Struct. **43**(14–15), 4047–4062 (2006)
75. Berdichevsky, V.L.: Variational Principles of Continuum Mechanics: I. Fundamentals. Springer, Heidelberg (2009)
76. dell'Isola, F., Di Cosmo, F.: Lagrange Multipliers in Infinite-Dimensional Systems, Methods of. In: Altenbach, H., Öchsner, A. (eds.) Encyclopedia of continuum mechanics, pp. 1432–1440. Springer, Berlin, Heidelberg (2020)
77. Bersani, A.M., dell'Isola, F., Seppecher, P.: Lagrange Multipliers in Infinite Dimensional Spaces, Examples of Application. In: Altenbach, H., Öchsner, A. (eds.) Encyclopedia of continuum mechanics, pp. 1425–1432. Springer, Berlin, Heidelberg (2020)
78. Courant, R., Hilbert, D.: Methods of Mathematical Physics, vol. 1. Wiley, New York (1991)
79. Collatz, L.: Eigenwertaufgaben Mit Technischen Anwendungen. Akademische Verlagsgesellschaft Geest & Portig, Leipzig (1963)
80. Gould, S.H.: Variational Methods for Eigenvalue Problems: an Introduction to the Weinstein Method of Intermediate Problems. Oxford University Press, London (1966)
81. Eremeyev, V.A., Lebedev, L.P., Cloud, M.J.: The Rayleigh and Courant variational principles in the six-parameter shell theory. Math. Mech. Solids **20**(7), 806–822 (2015)
82. Ladyzhenskaya, .A.: The Boundary Value Problems of Mathematical Physics. Applied Mathematical Sciences, vol. 49. Springer, New York (1985)
83. Thompson, J.M.T., Hunt, G.W.: Comparative perturbation studies of the elastica. Int. J. Mech. Sci. **11**(12), 999–1014 (1969)
84. Eremeyev, V.A.: On well-posedness of the first boundary-value problem within linear isotropic Toupin-Mindlin strain gradient elasticity and constraints for elastic moduli. ZAMM-Journal of Applied Mathematics and Mechanics/Zeitschrift für Angewandte Mathematik und Mechanik **103**(6), 202200474 (2023)
85. Challamel, N., Atashipour, S.R., Girhammar, U.A., Barroso, V.S., Andrade, A., Boutin, C., Eremeyev, V.A.: A historical overview on static and dynamic analyses of sandwich or partially composite beams and plates. Math. Mech. Solids **30**(7), 1608–1643 (2025)
86. Gibson, L.J., Ashby, M.F.: Cellular Solids: Structure and Properties, 2nd edn. Cambridge Solid State Science Series. Cambridge University Press, Cambridge (1997)
87. Askes, H., Metrikine, A.V.: One-dimensional dynamically consistent gradient elasticity models derived from a discrete microstructure: Part 2: Static and dynamic response. European Journal of Mechanics-A/Solids **21**(4), 573–588 (2002)
88. Truskinovsky, L., Vainchtein, A.: Quasicontinuum modelling of short-wave instabilities in crystal lattices. Phil. Mag. **85**(33–35), 4055–4065 (2005)
89. Michelitsch, T.M., Gitman, I.M., Askes, H.: Critical wave lengths and instabilities in gradient-enriched continuum theories. Mech. Res. Commun. **34**(7–8), 515–521 (2007)
90. Nejadsadeghi, N., Hild, F., Misra, A.: Parametric experimentation to evaluate chiral bars representative of granular motif. Int. J. Mech. Sci. **221**, 107184 (2022)
91. Barchiesi, E., dell'Isola, F., Seppecher, P., Turco, E.: A beam model for duoskelion structures derived by asymptotic homogenization and its application to axial loading problems. European Journal of Mechanics-A/Solids **98**, 104848 (2023)
92. Sougleridis, I.I., Brun, M., Baldi, A., Carta, G.: Microstructured tunable media with giant negative and positive thermal expansion. Journal of the Mechanics and Physics of Solids, 106373 (2025)

93. Eremeyev, V.A., Ganghoffer, J.-F., Konopińska-Zmysłowska, V., Uglov, N.S.: Flexoelectricity and apparent piezoelectricity of a pantographic micro-bar. Int. J. Eng. Sci. **149**, 103213 (2020)
94. Malikan, M., Wiczenbach, T., Eremeyev, V.A.: Thermal buckling of functionally graded piezomagnetic micro-and nanobeams presenting the flexomagnetic effect. Continuum Mech. Thermodyn. **34**(4), 1051–1066 (2022)
95. Polyanin, A.D., Zaitsev, V.F.: Handbook of Exact Solutions for Ordinary Differential Equations. CRC Press, Boca Raton (1995)

Publisher's Note Springer Nature remains neutral with regard to jurisdictional claims in published maps and institutional affiliations.